PAPER

Strong-field atomic physics meets ^{229}Th nuclear physics

IOP Publishing Journal of Physics B: Atomic, Molecular and Optical Physics
J. Phys. B: At. Mol. Opt. Phys. **54** (2021) 244001 (10pp) https://doi.org/10.1088/1361-6455/ac45ce

Strong-field atomic physics meets ^{229}Th nuclear physics

Wu Wang[1], Hanxu Zhang[2] and Xu Wang[2,*]

[1] Beijing Computational Science Research Center, Beijing 100193, People's Republic of China
[2] Graduate School, China Academy of Engineering Physics, Beijing 100193, People's Republic of China

E-mail: xwang@gscaep.ac.cn

Received 20 September 2021, revised 19 November 2021
Accepted for publication 22 December 2021
Published 11 February 2022

Abstract

We show how two apparently unrelated research areas, namely, strong-field atomic physics and ^{229}Th nuclear physics, are connected. The connection is possible due to the existence of a very low-lying excited state of the ^{229}Th nucleus, which is only about 8 eV above the nuclear ground state. The connection is physically achieved through an electron recollision process, which is the core process of strong-field atomic physics. The laser-driven recolliding electron is able to excite the nucleus, and a simple model is presented to explain this recollision-induced nuclear excitation process. The connection of these two research areas provides novel opportunities for each area and intriguing possibilities from the direct three-partite interplay between atomic physics, nuclear physics, and laser physics.

Keywords: recollision, strong-field atomic physics, thorium-229, isomeric states

(Some figures may appear in colour only in the online journal)

1. Introduction

Strong-field atomic physics studies the interaction between intense laser fields and isolated (gas-phase) atoms. It is a research area driven by intense-laser technologies, especially after the invention of the chirped pulse amplification technique [1]. The response of atoms to intense external laser fields is highly nonlinear and nonperturbative, extending traditional nonlinear optics into a new regime. Many new phenomena happen, such as multiphoton ionization [2–4], above-threshold ionization [5–7], high harmonic generation [8–10], nonsequential double or multiple ionization [11–13], laser-induced electron diffraction [14–16], etc. One of the most promising products of strong-field atomic physics is the generation of attosecond (1 as $= 10^{-18}$ s) light pulses [17], the shortest pulses generated currently being around 50 as [18–20]. The prospect is a new ultrafast temporal frontier following electronic motions inside an atom.

Thorium (Th) is the 90th element on the periodic table and ^{229}Th is one of its isotopes. What is special about this particular isotope is that the nucleus of ^{229}Th has a unique low-lying excited state, called an isomeric state, of energy around 8 eV above the nuclear ground state [21–25]. This is the lowest nuclear excite state among all known nuclei. The existence of this isomeric state has fascinated the scientific community for its potentiality as a 'nuclear clock' [26–29], which may complement or even outperform currently available atomic clocks. Other potential applications of this isomeric state include nuclear lasers [30], measuring variations of fundamental constants [31–33], etc.

Strong-field atomic physics and ^{229}Th nuclear physics, as briefly introduced above, appear to be two distinct and unrelated research areas, one being a subfield of atomic physics and the other being a subfield of nuclear physics. Yet they are connected. The essential reason for this connection is the low energy of the nuclear isomeric state: 8 eV, being a nuclear energy gap, lies within the energy range of electronic transitions. The connection is physically achieved via an electron recollision process, which is the core process of strong-field atomic physics unifying various strong-field phenomena, as will be explained in the following section.

In this article, we will first give a brief explanation to the recollision process. Then we will give a more elaborated introduction to the ^{229}Th nucleus, including its properties, poten-

* Author to whom any correspondence should be addressed.

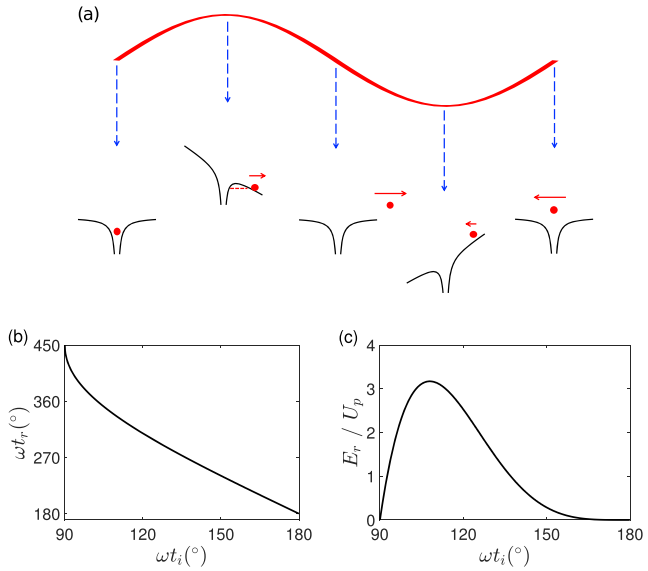

Figure 1. (a) Schematic illustration of the recollision process. (b) The relationship between the recollision time t_r and the emission time t_i. (c) The relationship between the recollision energy E_r and the emission time t_i. E_r is given in units of the ponderomotive energy U_p.

tial applications, and current research status. These materials are probably needed for the J. Phys. B readers who may not be familiar with this branch of nuclear physics. Next we will explain how these two research areas are connected by the recollision process. We use a simple, physically oriented, model to estimate the excitation rate of the nuclear isomeric state by laser-driven recolliding electrons. Outlooks on new opportunities for both research areas will be followed. A conclusion will be given at the end.

2. The recollision process and strong-field atomic physics

The interaction between intense laser fields and isolated atoms (or molecules) leads to many new phenomena that do not happen with weak laser fields, as mentioned above. The core physical process underlying these phenomena is the electron recollision process [34–37].

The recollision process is schematically illustrated in figure 1(a). The laser electric field oscillates so the total potential (atomic Coulomb potential plus laser electric potential) felt by an electron tilts with time, half cycle to the right and the other half cycle to the left. Ionization most probably happens around field peaks when the total potential is most tilted, via quantum tunneling through the formed potential barrier [38, 39]. The emitted electron is then driven away by the laser electric field. When the oscillating electric field reverses its direction, there are chances that the electron is driven back to and recollide with its parent ion core. During its excursion in the continuum, the electron may have gained some energy from the laser field and this determines how fast the returning electron will hit the ion core.

To get a more quantitative understanding about the recollision process, let us start from a simplified model (in fact we will be presenting the so-called 'simple-man' model [40] that has been extremely useful in understanding strong-field atomic phenomena, especially after the publication of [36]). We neglect for the time being the atomic Coulomb potential and consider the effect of the laser electric potential on a free electron. Suppose the laser field is linearly polarized along the z direction

$$\boldsymbol{E}(t) = \hat{z}E_0 \sin \omega t, \tag{1}$$

where E_0 is the amplitude and ω is the angular frequency. A long-wavelength approximation has been made which neglects spatial dependency of the laser electric field. Suppose an electron is emitted at some time t_i with zero initial velocity $v(t_\mathrm{i}) = 0$ and at position $z(t_\mathrm{i}) = 0$. Then the velocity of the electron at a later time t is

$$v(t) = -\int_{t_\mathrm{i}}^{t} E_0 \sin \omega t' \, dt' = \frac{E_0}{\omega}\left(\cos \omega t - \cos \omega t_\mathrm{i}\right). \tag{2}$$

Atomic units have been used with the mass of the electron $m = 1$ a.u. and the charge of the electron $q = -e = -1$ a.u. One can see that the velocity contains an oscillatory part and a drift part. The subsequent position of the electron can be calculated as

$$\begin{aligned} z(t) &= \int_{t_\mathrm{i}}^{t} v(t')dt' \\ &= -\frac{E_0}{\omega}(t - t_\mathrm{i})\cos \omega t_\mathrm{i} + \frac{E_0}{\omega^2}\left(\sin \omega t - \sin \omega t_\mathrm{i}\right). \end{aligned} \tag{3}$$

We look for time t that fulfills the recollision condition $z(t) = z(t_\mathrm{i}) = 0$, or more explicitly from the previous equation

$$\omega(t - t_\mathrm{i})\cos \omega t_\mathrm{i} = \sin \omega t - \sin \omega t_\mathrm{i}. \tag{4}$$

This equation does not always have a solution. It turns out that if the electron is emitted before a field peak, e.g. $0^\circ < \omega t_\mathrm{i} < 90^\circ$, the above equation has no solution and the electron will not recollide. The electron will recollide if it is emitted on or after a field peak, e.g. $90^\circ \leqslant \omega t_\mathrm{i} < 180^\circ$. The solved recollision time is noted as t_r. The relationship between t_r and t_i is plotted in figure 1(b). Note that there may be more than one t_r for some t_i values, corresponding to higher-order recollisions. These recollisions are usually negligible for the following two reasons. First, if the ionic Coulomb potential were considered, the electron would be scattered to other directions without the chance of a second recollision. Second, if the transverse spreading of the electron wavepacket were considered, then higher-order recollisions would lead to more severe wavepacket spreading hence less contributions to recollision-induced processes.

Putting the solved $\{t_\mathrm{r}, t_\mathrm{i}\}$ pairs into equation (2) one gets the velocity and kinetic energy of the electron at the time of recollision. It can be found numerically that if the electron is emitted at $\omega t_\mathrm{i} = 107^\circ$, then the recollision energy E_r is maximum with a value of $3.17U_\mathrm{p}$. Here $U_\mathrm{p} = E_0^2/4\omega^2$ denotes the ponderomotive energy, which is the cycle-averaged kinetic energy of a free electron in the laser field. The relationship between E_r and t_i is given in figure 1(c).

Most strong-field processes are closely related to recollision. The recolliding electron may (1) recombine with its parent ion core radiatively leading to high harmonic generation [8–10]; or (2) kick out another bound electron(s) leading to nonsequential double (multiple) ionization [11–13]; or (3) be scattered elastically leading to laser-induced electron diffraction [14–16]. With typical laser intensities (10^{14} to 10^{16} W cm^{-2}) in strong-field atomic physics, the recollision energy of the electron is usually several tens to a few hundreds of electronvolts. The recolliding electron usually does not have an effect on the nucleus, the energy scale of which is typically on the order of 1 MeV. With the ^{229}Th nucleus, however, a new possibility is within sight. The recolliding electron has enough energy to excite the ^{229}Th nucleus from the ground state to the isomeric state. This possibility, on the one hand, expands the realm of strong-field atomic physics, and on the other hand, provides a new approach for the isomeric excitation of the ^{229}Th nucleus. This new approach has unique advantages compared with existing excitation approaches, as will be explained later.

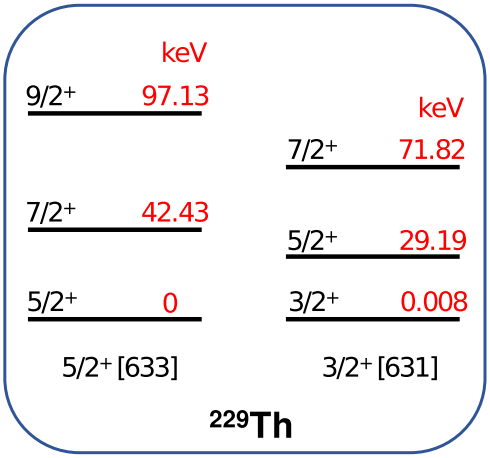

Figure 2. The first few energy levels of the ^{229}Th nucleus. These levels belong to two rotational bands, with the ground state the band head of the $5/2^+$ band (Nilsson quantum numbers [633]) and the isomeric state the band head of the $3/2^+$ band (Nilsson quantum numbers [631]). The energy value (in keV) of each state is shown in red.

3. The isomeric state of the ^{229}Th nucleus

In this section we shall give a more detailed introduction to the isomeric state of the ^{229}Th nucleus, as well as the current status of research. The existence of a low-lying isomeric state in ^{229}Th was first proposed in 1976 by Kroger and Reich by analyzing the γ radiation following α decay of ^{233}U [21]. The energy of the isomeric state was identified to be less than 100 eV. It was then determined to be -1 ± 4 eV [22], 3.5 ± 1.0 eV [23], 7.6 ± 0.5 eV [24], and most recently 8.28 ± 0.17 eV [25].

The first few energy levels of the ^{229}Th nucleus are shown in figure 2. The ground state and the isomeric state belong to two different rotational bands: the former is the band head of a $5/2^+$ band (5/2 is the projection of the total angular momentum on a symmetry axis, and the plus sign means positive parity of the state), and the latter is the band head of a $3/2^+$ band [21]. The energies of the two band heads happen to be very close to each other, which is quite a (fortunate) coincidence.

The existence of a nuclear energy gap in the optical regime (photon energy 8 eV = wavelength 155 nm) is fascinating. First, the possibility emerges of using lasers to directly manipulate the quantum state of the nucleus. Lasers have been powerful tools of manipulating quantum states of atoms or molecules, yet they have not played a similar role in nuclear physics due to the vast gap between laser photon energies and (typical) nuclear energy gaps. This possibility is now open with ^{229}Th, at least energetically. Second, the nuclear degree of freedom can be efficiently coupled to the electronic degree of freedom. Electronic states or energy gaps are also on the 1 eV order of magnitude. Therefore the ^{229}Th atom provides a rare platform where atomic physics, nuclear physics, and laser physics directly interplay. It would be intriguing to see the possibilities from this three-partite interplay.

The isomeric state has been proposed as a potential nuclear clock that may outperform current state-of-the-art electronic-shell-based atomic clocks [26–29]. This is mainly due to the reason that the linewidth of the isomeric state is very narrow ($\Delta E/E \approx 10^{-20}$) and that the nucleus is much less affected by environmental perturbations than the electrons. The nuclear clock may perform with a total fractional inaccuracy on the level of 10^{-19}, which is two orders of magnitude better than state-of-the-art atomic clocks [29]. Proposal has also been made of a nuclear laser exploiting this isomeric state. Several population inversion schemes are proposed making use of level splittings of the isomeric state and the ground state [30]. The high precision of the nuclear clock may be used to search for variations of fundamental constants, such as the fine structure constant $\alpha = e^2/\hbar c$ and the dimensionless strong interaction parameter $m_{q,e}/\Lambda_{QCD}$ [31–33]. Here Λ_{QCD} is the quantum chromodynamics scale, and m_q (m_e) is the quark (electron) mass.

Substantial progresses have been made in the past few years in characterizing the isomeric state. The energy of the isomeric state has been determined using a new approach [25, 41]. Previous determinations of the energy are based on γ-ray spectroscopy following α decay of ^{233}U [21–24, 42, 43]. The new approach is based on an internal conversion process [25, 41], in which the nucleus decays from the isomeric state to the ground state and transfers the energy to free a bound electron. The magnetic dipole moment, the electric quadrupole moment, and the charge radius of the isomeric state have been determined via hyperfine spectroscopy [44, 45].

To realize the above-mentioned exciting applications, the first step is to prepare, or generate, the isomeric state, preferably in a controllable and efficient way. Naturally the isomeric state can be generated from α decay of ^{233}U ($^{233}\text{U} \rightarrow {}^{229}\text{Th} + \alpha$, half-life 1.592×10^5 years), with 2% of the resultant ^{229}Th nuclei in the isomeric state. This decay, however, is largely uncontrollable. The ^{229}Th nuclei are left with a recoil energy of 84 keV into random directions and various ionic states. The efficiency is not high either. One can estimate from the

half-life and the branching ratio that every 3.6×10^{14} ^{233}U nuclei generate a single ^{229}Th nucleus in the isomeric state per second.

Direct (vacuum ultraviolet, VUV) light excitation from the nuclear ground state seems to be the most straightforward approach. Such VUV light can be generated from synchrotron facilities or from high harmonic generation with 800 nm Ti:sapphire lasers. Several attempts have been made to optically excite the ^{229}Th nucleus and detect the subsequent light emission. However, no evidence has been found for the anticipated transition [46–49]. Possible reasons include inaccurate knowledge of the isomeric energy, background radiations with similar frequencies, competition with non-radiative relaxation processes, etc.

Another excitation approach based on electronic bridge (EB) processes has been proposed with various ionic states or doped-crystal systems [50–53]. The idea is to couple the nuclear degree of freedom to the electronic degree of freedom. The energy released from an electronic transition (e.g. from an excited electronic state to the ground state) may transfer to and excite the nucleus. The energy mismatch between the electronic transition and the nuclear isomeric transition is compensated by an external laser field with the required frequency. Although extensively studied theoretically, the EB approach has not been realized experimentally due to its sophisticated requirements on experimental conditions. Both the energy of the isomeric state and the electronic structures of the involved ^{229}Th ions need to be known with high precision.

Up to now the only experimentally demonstrated excitation of the isomeric state uses an indirect light excitation approach [54]. The ^{229}Th nucleus is first pumped to the 29 keV second excited state (see figure 2) using synchrotron radiation. The second excited state then decays (half-life about 100 ps) preferably into the isomeric state. This approach relies on narrowband and high-photon-energy synchrotron facilities, which are not easily accessible.

From the above summary one can see that new approaches are still highly desirable that can generate the isomeric state controllably and efficiently. The new approaches should be easy to implement experimentally and preferably without the requirement of big facilities like synchrotron. Interestingly, the combination of ^{229}Th nuclear physics and strong-field atomic physics leads to a new excitation approach that satisfies these conditions.

4. Using recollision to excite the isomeric state of ^{229}Th

The idea is inspired to use laser-driven recolliding electrons to excite the ^{229}Th nucleus. Let us call this new approach recollision-induced nuclear excitation (RINE) [55]. One can see that the RINE approach also exploits on the coupling between the electronic degree of freedom and the nuclear degree of freedom. It is to be noted that the electronic states involved are mostly continuum states instead of discrete states. This is also one of the major differences between strong-field atomic physics and other branches of atomic physics.

In this section we will present a simple, physically oriented, model of the RINE process and estimate the efficiency. The model incorporates electronic excitation cross sections of the nucleus, calculated quantum mechanically with approximations, and the flux density of the recolliding electrons, calculated from a classical-trajectory simulation. The advantages of this semi-classical model include a clear physical picture and a simple theoretical formalism. A full quantum mechanical calculation is desirable, which, however, would be much more complicated in both formalism and computation.

Consider a neutral ^{229}Th atom in the presence of a femtosecond laser pulse. As the laser pulse turning on, an electron is pulled out from the atom at time t_i and later driven back to recollide with the remaining ion core and excite the nucleus at time t_r. The nuclear excitation rate is the product of the electronic excitation cross section and the recolliding electron flux

$$\Gamma(t_\mathrm{r}) = \sigma(E_\mathrm{r}) j(t_\mathrm{r}). \tag{5}$$

Recall that the dependencies of the recollision time t_r and the recollision energy E_r on the emission time t_i have been shown in figure 1. The cross section $\sigma(E_\mathrm{r})$ is a property of the ^{229}Th nucleus, and the recolliding-electron flux $j(t_\mathrm{r})$ is determined by the interaction between the ^{229}Th atom and the laser field. Therefore the above equation tells exactly the combination between ^{229}Th nuclear physics and strong-field atomic physics.

4.1. The electronic excitation cross section

The electronic excitation cross section of nuclei has been treated in the literature, e.g. in the classic article of Alder *et al* [56]. Without repeating the derivations, we only list some final formulas here. For the ^{229}Th nucleus, the electric dipole ($E1$) transition is forbidden due to a parity consideration. The leading terms are the electric quadrupole ($E2$) and the magnetic dipole ($M1$) transitions. The differential cross section for the $E2$ transition is given as

$$\frac{d\sigma_{E_2}}{d\Omega} = \frac{2\pi}{75c^2} B(E2) \frac{K^4}{k_\mathrm{i}^2} \left(V_\mathrm{T} + \frac{2}{3} V_\mathrm{L} \right), \tag{6}$$

and the differential cross section for the $M1$ transition is given as

$$\frac{d\sigma_{M_1}}{d\Omega} = \frac{8\pi}{9c^2} B(M1) \frac{K^2}{k_\mathrm{i}^2} V_\mathrm{T}. \tag{7}$$

In the above formulas, c is the speed of light, $\boldsymbol{k}_\mathrm{i}$ ($\boldsymbol{k}_\mathrm{f}$) is the initial (final) wave vector of the electron, and $\boldsymbol{K} = \boldsymbol{k}_\mathrm{i} - \boldsymbol{k}_\mathrm{f}$ is the momentum transfer in the collision. $B(E2)$ and $B(M1)$ are the so-called reduced transition probabilities of the corresponding channel, the values of which are determined experimentally or through theoretical calculations. V_T and V_L are wave vector-dependent functions given by

$$V_\mathrm{T} = k_\mathrm{i} k_\mathrm{f} \frac{(k_\mathrm{i}^2 + k_\mathrm{f}^2 - \kappa^2) K^2 - 2(\boldsymbol{k}_\mathrm{i} \cdot \boldsymbol{K})(\boldsymbol{k}_\mathrm{f} \cdot \boldsymbol{K})}{K^2 (K^2 - \kappa^2)^2}, \tag{8}$$

$$V_\mathrm{L} = k_\mathrm{i} k_\mathrm{f} \frac{2k_\mathrm{i}^2 + 2k_\mathrm{f}^2 + 4c^2 - \kappa^2 - K^2}{K^4}, \tag{9}$$

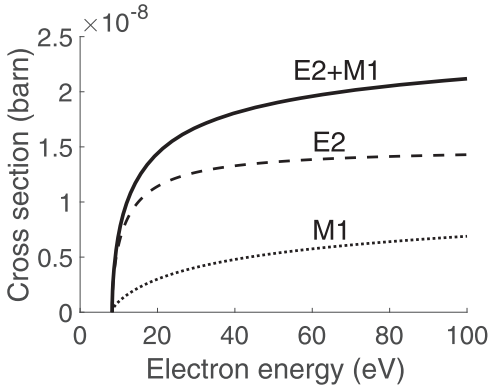

Figure 3. Excitation cross section of the isomeric state of ^{229}Th by electrons, for the $E2$ channel (dashed) and the $M1$ channel (dotted). The sum of these two channels is shown as the solid curve.

where $\kappa = \Delta E/c$ with ΔE the energy transfer (i.e. the energy difference between the isomeric state and the ground state).

The total cross section σ_{E2} and σ_{M1} can be obtained by integrating over the solid angle dΩ. Figure 3 shows the total cross section for these two channels as a function of the electron energy. The following points are noted: (1) we have used the reduced transition probabilities $B(E2) = 27$ W.u. (Weisskopf units) and $B(M1) = 0.0076$ W.u. as suggested theoretically in [57], although newer values have been suggested by the same authors [58]. The newer values of $B(E2)$ are between 30 and 50 W.u. and those of $B(M1)$ are between 0.005 and 0.008 W.u. If these values were used, the total $E2 + M1$ cross sections would be somewhat higher than the results presented in figure 3. (2) The cross section formulas given above are based on the Born approximation, which assumes plane waves for the spatial part of the electronic wave function. Experiences from quantum mechanical calculations usually find the Born approximation underestimating the cross sections. More accurate cross sections are of course highly desirable.

4.2. The flux density of the recolliding electron

To estimate the excitation rate given in equation (5), we also need to know the flux density of the recolliding electron(s) at each time. The quantum mechanical approach would be to solve a time-dependent Schrödinger equation describing the interaction between the ^{229}Th atom and the laser field, and to extract carefully the wave packet and the flux density of the recolliding electron. This approach is rather tedious and the computational load is high. Here, we use a much simpler approach. We estimate the flux density using a classical trajectory simulation that is widely employed in strong-field atomic physics to describe the evolution of an emitted electron [59–69].

At each time, there is a chance that an electron is emitted via quantum tunneling. The rate of tunneling ionization can be estimated using an Ammosov–Delone–Krainov (ADK) tunneling formula [39]

$$w(t) = \frac{f(l,m)}{\kappa^{2Z_c/\kappa-1}}\left(\frac{2\kappa^3}{|E(t)|}\right)^{2Z_c/\kappa-|m|-1} e^{-2\kappa^3/3|E(t)|}. \qquad (10)$$

Here l and m are the angular quantum numbers of the ionized atomic state, $\kappa = \sqrt{2I_p}$ with I_p the ionization potential, Z_c is the charge of the ion core seen by the emitted electron, and $E(t)$ is the laser electric field. The coefficient $f(l,m)$ is given by

$$f(l,m) = \frac{C_l^2}{2^{|m|}|m|!}\frac{(2l+1)(l+|m|)!}{2(l-|m|)!}, \qquad (11)$$

where C_l is a constant on the order of unity in atomic units. There has been no study reporting the values of C_l particularly for ^{229}Th, so we take $C_l = 1$ a.u. for the time being. Reported values of C_l are mostly between 1 and 3 a.u. for rare gas atoms (which are the commonly used targets in strong-field atomic physics) [39]. The ionization probability is then given as

$$P_{\rm ion}(t) = 1 - \exp\left[-\int_{t_0}^{t} w(t')dt'\right], \qquad (12)$$

where t_0 is the time when the laser pulse starts.

After the electron is emitted, we assume that it propagates according to classical mechanics. The emitted electron feels a potential from the nucleus and from the remaining electrons. If the electron is the first- (second-, third-, …) emitted electron, it sees 89 (88, 87, …) remaining electrons. We use an effective potential to describe the potential seen by the emitted electron

$$V(r) = \frac{1}{r}\left[-(Z-N) - \frac{N}{(e^{r/d}-1)\xi+1}\right], \qquad (13)$$

where $Z = 90$ is the charge number of the nucleus, and N (=89, 88, 87, …) is the number of the remaining electrons. The two parameters d and ξ take values 0.927 and 5.58 a.u., respectively. This form of effective potentials was given by Green, Sellin, and Zachor in reference [70] and has been widely used in atomic physics with the abbreviated name the GSZ potential.

To propagate the trajectory of the emitted electron, one also needs initial conditions, including the position and the momentum (velocity) at the time of emission. The initial position of the electron, i.e. the tunneling-exit point, is determined by equating the total potential of the electron to the negative of the ionization energy

$$V(r) + E(t_i)z = -I_p. \qquad (14)$$

In writing the above equation, we have assumed that the laser field is linearly polarized along the z axis. $V(r)$ is the GSZ potential and t_i is the time of ionization. I_p could be I_{p1} (6.3 eV), I_{p2} (12.1 eV), I_{p3} (18.3 eV),…, depending on the number of remaining electrons. Assuming that the electron is emitted on the polarization axis, i.e. $r = |z|$, the above equation (14) can be solved numerically which gives the initial position of the electron at the emission time t_i.

The longitudinal momentum (i.e. momentum along the laser polarization direction) of the electron at the tunneling exit is usually assumed to be zero from a classical argument: the tunneling exit is the position where the kinetic energy, hence the momentum, vanishes, although some studies also argue for slightly nonzero longitudinal momenta [71–76]. The transverse momentum (i.e. momentum perpendicular to the laser

polarization direction) of the electron at the tunneling exit is shown to have a Gaussian distribution [77]

$$P(v_\perp) \propto \exp\left(-\frac{v_\perp^2}{\eta^2}\right) \tag{15}$$

with $\eta^2 = |E(t)|/\sqrt{2I_p}$.

With the initial conditions given, the subsequent trajectory of an emitted electron is determined classically via integrating the Hamiltonian equations of motion

$$\frac{dr_i}{dt} = \frac{\partial H}{\partial p_i}; \tag{16}$$

$$\frac{dp_i}{dt} = -\frac{\partial H}{\partial r_i}, \tag{17}$$

where $i = x, y, z$, and $H = (p_x^2 + p_y^2 + p_z^2)/2 + V(r) + zE(t)$. We integrate the above equations using the Livermore solver for ordinary differential equations [78]. In our calculation we launch many trajectories to simulate a single emitted electron. The laser pulse is divided into small time steps with $\Delta t = 0.1$ a.u. (For 800 nm, one laser cycle is about 110 a.u.) At each time step 10^5 trajectories are initiated at the tunneling exit point (which changes from time to time) with zero longitudinal velocities but randomly assigned transverse velocities (Convergence has been checked by doubling the number of trajectories). A weight is assigned to each trajectory, according to the ADK rate of equation (10) and the Gaussian transverse-velocity distribution of equation (15). The total weight of the 10^5 trajectories initiated at time t_i is set to be $w(t_i)\Delta t[1 - P_{ion}(t_i)]$, the value in the square bracket being the probability of survival at the time.

We follow each trajectory and determine whether it recollides, i.e. whether it passes through the $z = 0$ plane. If it does, we record its collision distance defined as $R_0 \equiv (x_0^2 + y_0^2)^{1/2}$ on the $z = 0$ plane. The recolliding electron flux is not uniformly distributed on the $z = 0$ plane. The range of R_0 can be estimated using the Gaussian transverse-velocity distribution and the excursion time $(t_r - t_i)$ of the recolliding electron. Obviously if R_0 is large, the corresponding trajectory interacts with the nucleus so slightly that nuclear excitation cannot happen. There exists a critical radius beyond which the recolliding trajectories do not contribute to the nuclear excitation. This critical radius of effective excitation can be estimated using the following procedure [56]: (1) each trajectory is followed with $r(t) = [x(t)^2 + y(t)^2 + z(t)^2]^{1/2}$ which provides a time-dependent interaction potential $V(t) = V[r(t)]$ using equation (13); (2) a Fourier transformation is performed on $V(t)$ and one looks particularly for the component $\tilde{V}(\omega_0) = \int_{-\infty}^{\infty} V(t)e^{-i\omega_0 t}\,dt$ with $\omega_0 = 8.3$ eV the energy of the isomeric state. This Fourier transformation comes from first-order perturbation theory, from the perspective of which the potential $V(t)$ is the time-dependent perturbation Hamiltonian that excites the nucleus. It follows that the temporal duration of a potential $V(t)$, noted δt, and the possible energy range of excitation, noted $\delta\omega$, satisfy an uncertainty relation $\delta t\delta\omega \approx 1$. $V(t)$ must change fast enough to have a substantial component at ω_0. A trajectory with a large R_0 changes too slowly to have the required component. The dependency of $|\tilde{V}(\omega_0)|^2$ on R_0 is shown in figure 4. This result is obtained for a single time step, but results from other time steps are quite similar. One sees that trajectories with $R_0 > 5$ a.u. do not contribute to the nuclear excitation. Trajectories with $R_0 < 1$ a.u. are most effective to the nuclear excitation.

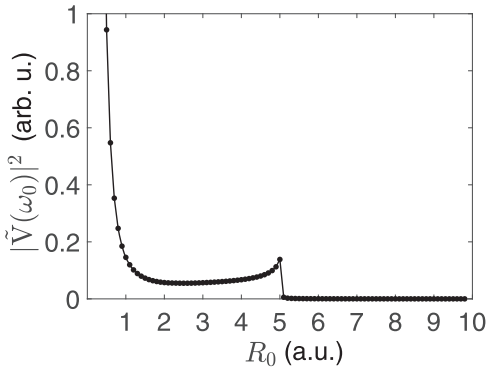

Figure 4. $|\tilde{V}(\omega_0)|^2$ as a function of the recollision distance R_0, where $\omega_0 = 8.3$ eV is the energy of the isomeric state.

The recolliding-electron flux density $j(t_r)$ in equation (5) can thus be estimated by summing over the weights of all trajectories that recollide at time t_r with $R_0 < 1$ a.u., then dividing the area of π a.u. With the excitation cross section $\sigma(E_r)$ and the recolliding-electron flux density $j(t_r)$, the instantaneous excitation rate $\Gamma(t_r)$ can be estimated at each recollision time t_r. Accumulating all the recollision times one can get the total excitation probability during the laser pulse.

4.3. The probability of nuclear excitation

Figure 5 shows the ionization probabilities and the nuclear isomeric excitation probabilities for a neutral ^{229}Th atom exposed to a laser pulse with peak intensity 10^{14} W cm^{-2} (top row) and 10^{15} W cm^{-2} (bottom row). Accumulated probabilities are shown during the laser pulse. The lower intensity is able to pull out three electrons from the ^{229}Th atom, as shown in figure 5(a). Ionizations of the first two electrons are complete and that of the third electron is partial. Ionization of the fourth electron is negligible. Each of the three electrons has chances to be pulled back to recollide with the ion core and excite the nucleus, and the contribution from each electron to the nuclear isomeric excitation can be calculated separately using the method explained in the previous section. The isomeric excitation probabilities are shown in figure 5(b). Note that only the second and the third electrons contribute to the isomeric excitation. This is because the first electron has a very low ionization potential ($I_{p1} = 6.3$ eV), and it is emitted too early during the laser pulse and does not have enough recollision energy to excite the nucleus. In contrast, the second and the third electrons do have enough recollision energy to excite the nucleus. The nuclear isomeric excitation probability is estimated to be on the order of 10^{-18}.

With the higher intensity of 10^{15} W cm^{-2}, the laser is able to pull out four electrons, as shown in figure 5(c). Ionization of the fifth electron is negligible with this intensity. Similarly the first electron does not contribute to the nuclear excitation. The second, third, and fourth electrons contribute to the nuclear

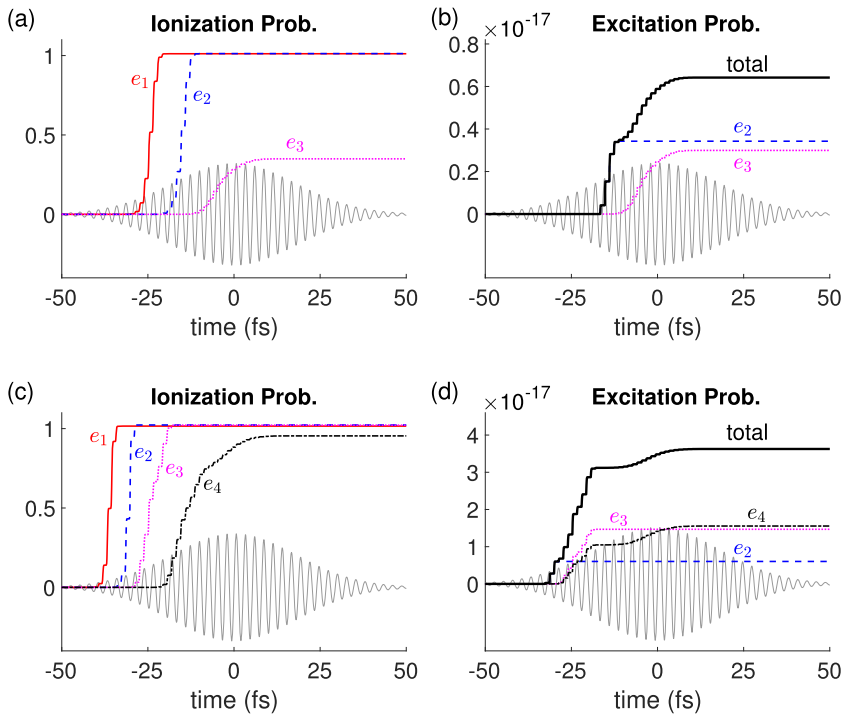

Figure 5. Ionization probabilities (left column) and nuclear isomeric excitation probabilities (right column) for a neutral ^{229}Th atom exposed to a laser pulse of peak intensity 10^{14} W cm^{-2} (top row) and 10^{15} W cm^{-2} (bottom row). Probabilities from each individual electron are separately labeled. The laser pulses are assumed to have a Gaussian temporal shape with duration 30 fs. The temporal shape of the laser electric field is shown in each figure as background.

excitation as shown in figure 5(d). The contributions from the third electron and the fourth electron are similar in amount, higher than the contribution from the second electron. This is mainly due to higher recollision energies hence higher excitation cross sections from these electrons. The total excitation probability is on the order of 10^{-17}, about six times higher than the lower-intensity case.

The above estimations consider the probability of nuclear excitation for a single ^{229}Th atom exposed to a single laser pulse. The production rate of our RINE approach depends on the number of ^{229}Th atoms that are effectively radiated by each pulse, noted as N_0, and the laser repetition rate. The state-of-the-art repetition rate that can be achieved by current intense laser systems is about 100 kHz [79–82]. The number N_0 depends on the number density of ^{229}Th atoms and the laser focal volume. In the following we give an estimation to these two qualities.

Consider ^{229}Th in the gas phase, with which the atomic physics discussed above is valid. Laser pulses ionize the atoms and turn the gas into a plasma. For continuous operation the density of the freed electrons must be below the critical density $n_{\rm cr}$, otherwise the laser will crease to propagate. This sets an upper limit of the number density of the ^{229}Th atoms. Since each atom may be ionized 3 or 4 times as shown in figure 5, the maximum number density of the atoms is $n_{\rm cr}/4$. To be safer let us use $n_{\rm cr}/10$ as an estimation of the atom density. From plasma physics $n_{\rm cr} = m\epsilon_0\omega^2/e^2 = 1.7 \times 10^{21}$ cm^{-3} for 800 nm lasers (m: electron mass; ϵ_0: vacuum permittivity; ω: laser angular frequency; e: electron charge), so the maximum atom density is estimated to be 1.7×10^{20} cm^{-3}.

The focal volume can be estimated using a Gaussian beam profile with $V_{\rm foc} = \pi w_0^2 \times 2Z_{\rm R}$, where w_0 is the beam waist on the focal plane and $Z_{\rm R} = \pi w_0^2/\lambda$ is the Rayleigh length. For a Gaussian temporal dependency the focal volume can also be written as

$$V_{\rm foc} = \frac{16E_L^2}{\pi\lambda I_L^2 \tau_L^2}, \tag{18}$$

where E_L is the pulse energy, I_L is the peak intensity, and τ_L is the $(1/e^2)$ pulse duration. For example, for 800 nm wavelength, 30 fs pulse duration, and 0.1 mJ pulse energy, the focal volume is roughly 7×10^{-7} cm^{-3} for 10^{15} W cm^{-2}, and 7×10^{-5} cm^{-3} for 10^{14} W cm^{-2}. Using the above-obtained atom density, we can estimate the number of effectively radiated atoms N_0 to be 1.2×10^{14} for 10^{15} W cm^{-2}, and 1.2×10^{16} for 10^{14} W cm^{-2}.

The production rate per second of the excited nuclei can be estimated by $N_0\times$ [excitation probability per pulse] $\times$ [laser repetition rate, using 10^5 here]. For 10^{15} W cm^{-2}, let us use 10^{-17} as the excitation probability per pulse, and we get a production rate of 1.2×10^2 per second. For 10^{14} W cm^{-2}, let us use 10^{-18} as the excitation probability per pulse, and we get a production rate of 1.2×10^3 per second.

For a laser pulse with a certain energy, there exists an optimal focal size for nuclear excitation, due to the competition between the laser intensity and the focal volume. A smaller focal volume leads to higher intensities (hence higher excitation probabilities per pulse) but less radiated atoms, while a larger focal volume leads to lower intensities but more radiated atoms. The optimal focal size yields the best compromise

between the two. In the current case 10^{14} W cm^{-2} leads to a better compromise than 10^{15} W cm^{-2}. Further optimizations will not be pursued here, which merely require similar calculations with many laser intensities.

Our RINE approach only requires table-top laser systems [79–82]. Nevertheless we mention that much more energetic laser pulses (pulse energy $>$ 1 mJ) can be generated with the same repetition rate on big light facilities such as ELI-ALPS [83]. The nuclear excitation rate can be much higher using these energetic pulses.

4.4. Further remarks

We have explained the RINE process and estimated its efficiency using a simple semi-classical model. The model provides a clear physical picture of the RINE process and a simple theoretical formalism with very moderate computational loads. Nevertheless we want to reminder the readers about the approximations used in the model.

(a) We have used an electronic excitation cross section based on the Born approximation [56]. Although it is adequate for the current article to explain the physical process and provide a first estimate, the Born approximation is known to work better for high collision energies than for low collision energies. Further works are needed to obtain more precise electronic excitation cross sections for ^{229}Th beyond the Born approximation. With more precise cross sections the efficiency of the RINE method should be re-evaluated.

(b) We have estimated the recolliding-electron flux density using a classical trajectory simulation. Quantum mechanically one can solve a time-dependent Schrödinger equation describing the interaction between a ^{229}Th atom or ion and an external laser pulse, with the aid of a similar single-active-electron approximation that has been adopted in the classical simulation, treating the remaining ion core by an effective potential. The flux density can be extracted from the wave packet of the recolliding electron.

(c) We have neglected electron correlation effects in the classical trajectory simulation. When the trajectory of an emitted electron is propagated, the remaining electrons are modeled by an effective static potential. How would dynamical electron correlations affect the recollision process and the recolliding flux density remains to be studied.

5. New opportunities for each research area

The connection between strong-field atomic physics and ^{229}Th nuclear physics, through the electron recollision process, leads to new research opportunities for each area.

The realm of strong-field atomic physics is expanded to include the nuclear degree of freedom. It is therefore desirable to see how this new degree of freedom can be controlled. For example, what laser wavelength would be better for the purpose of nuclear excitation? A longer wavelength leads to a higher recollision energy, which corresponds to a higher excitation cross section. Yet it also leads to a more severe wave packet spreading along the transverse direction hence a lower recollision flux density. There should be a range of wavelengths that work better for nuclear excitation compromising these two factors. For another example, going beyond the single-color sinusoidal wave, would a superposition of two or three colors (with appropriate relative intensity and relative phase) work better for nuclear excitation? Similar waveform optimizations have been successful in optimizing or controlling high harmonic generation [84–87].

The RINE approach discussed here is a non-radiative process, the recolliding electron transferring energy to and exciting the nucleus without radiating photons. In fact, there exists a possible radiative-coupling channel [88]: the recolliding electron radiates high harmonic photons which then excite the nucleus. If the fundamental laser has a wavelength of 800 nm (photon energy 1.55 eV), the most relevant photons are the fifth harmonics with photon energies around 7.75 eV. Studies are needed to compare which type of electron–nucleus coupling, non-radiative or radiative, is more efficient in exciting the nucleus.

It would also be interesting to see possible correlations between the nuclear excitation process and other strong-field atomic processes, such as high harmonic generation, nonsequential double ionization, elastic electron scattering, etc. These processes are, after all, based on the same recollision process. If correlations could be found between nuclear excitation and atomic processes, then one might infer information about the nuclear excitation from observations of better-understood strong-field atomic processes.

In recent years, strong-field physics has also been extended to study the interaction between strong laser fields and solid-state targets. For example, generation of high harmonics is possible from this interaction [89–94]. Since ^{229}Th is naturally in the solid state, it would be interesting to see whether isomeric nuclear excitation can be achieved via the interaction between a strong laser field and solid-state ^{229}Th.

From the ^{229}Th nuclear physics point of view, the connection with strong-field atomic physics leads to an excitation approach with the following advantages, some of which are unique. (1) The new RINE approach does not require precise knowledge of the energy of the isomeric state, which is still uncertain by about 0.5 eV. This uncertainty in energy imposes a major difficulty for other excitation approaches that require a precise resonant condition, such as the EB approach, which has not been experimentally realized. In contrast, the property of the recolliding electron is that it has a wide energy range which certainly covers the (uncertain) energy of the isomeric state. (2) The new RINE approach does not require big facilities like synchrotron radiations. Instead, it only needs table-top laser systems which are much readily available. This makes the new approach much easier to implement and the available working time is much longer than the limited beam time from big facilities. (3) The nuclear excitation is very well timed which happens only within a fraction of a femtosecond laser pulse (see figure 5). This property may be essential for future coherent operations on the isomeric state. (4) After

the RINE process, the excited nuclei are accompanied with well controlled ionic states without subsequent decay via internal conversion. And the excited nuclei are left with negligible recoil energies.

The RINE scheme may also be applied to the ^{235}U nucleus, which has an isomeric state of energy 76 eV [95]. This energy is also within reach by laser-driven recolliding electrons. ^{229}Th and ^{235}U are the only two known nuclei with an excited state below 1 keV.

6. Conclusion

In this special issue article we have considered connections between two apparently unrelated research areas, namely strong-field atomic physics and ^{229}Th nuclear physics. These connections between a subfield of atomic physics and a subfield of nuclear physics are due to the existence of a very low-lying excited state of the ^{229}Th nucleus. The 8 eV nuclear energy gap lies within reach of electronic transitions, which can be efficiently manipulated by external laser fields. The ^{229}Th atom is a rare platform on which nuclear physics, atomic physics, and laser physics directly interplay.

Recollision is the physical process that connects these two research areas. It is the core process of strong-field atomic physics, unifying various strong-field phenomena, such as high harmonic generation, attosecond pulse generation, nonsequential double or multiple ionization, laser-induced electron diffraction, etc. With the ^{229}Th nucleus, the new RINE channel is energetically open, which adds a completely new degree of freedom to strong-field atomic physics. We have used a simple, physically oriented, model to explain the RINE process and estimate its efficiency.

The combination between strong-field atomic physics and ^{229}Th nuclear physics leads to novel opportunities for each research area, as we briefly envisaged in the previous section. It will be exciting to see new research results from this combination, and possible surprises from the three-partite interplay between nuclear physics, atomic physics, and laser physics. There is certainly much to be expected.

Acknowledgments

We acknowledge support from Science Challenge Project of China No. TZ2018005, NSFC No. 11774323 and No. 12088101, and NSAF No. U1930403.

Data availability statement

All data that support the findings of this study are included within the article (and any supplementary files).

ORCID iDs

Xu Wang https://orcid.org/0000-0002-8043-7135

References

[1] Strickland D and Mourou G 1985 *Opt. Commun.* **56** 219
[2] Voronov G and Delone N 1965 *JETP Lett.* **1** 66
[3] Agostini P, Barjot G, Bonnal J, Mainfray G, Manus C and Morellec J 1968 *IEEE J. Quantum Electron.* **4** 667
[4] Mainfray G and Manus G 1991 *Rep. Prog. Phys.* **54** 1333
[5] Agostini P, Fabre F, Mainfray G, Petite G and Rahman N K 1979 *Phys. Rev. Lett.* **42** 1127
[6] Kruit P, Kimman J, Muller H G and van der Wiel M J 1983 *Phys. Rev.* A **28** 248
[7] Paulus G G, Nicklich W, Xu H, Lambropoulos P and Walther H 1994 *Phys. Rev. Lett.* **72** 2851
[8] McPherson A, Gibson G, Jara H, Johann U, Luk T S, McIntyre I A, Boyer K and Rhodes C K 1987 *J. Opt. Soc. Am.* B **4** 595
[9] Ferray M, L'Huillier A, Li X F, Lompre L A, Mainfray G and Manus C 1988 *J. Phys. B: At. Mol. Opt. Phys.* **21** L31
[10] Seres J *et al* 2005 *Nature* **433** 596
[11] Walker B, Sheehy B, DiMauro L F, Agostini P, Schafer K J and Kulander K C 1994 *Phys. Rev. Lett.* **73** 1227
[12] Palaniyappan S, DiChiara A, Chowdhury E, Falkowski A, Ongadi G, Huskins E L and Walker B C 2005 *Phys. Rev. Lett.* **94** 243003
[13] Becker W, Liu X, Ho P J and Eberly J H 2012 *Rev. Mod. Phys.* **84** 1011
[14] Morishita T, Le A T, Chen Z J and Lin C D 2008 *Phys. Rev. Lett.* **100** 013903
[15] Blaga C I, Xu J, DiChiara A D, Sistrunk E, Zhang K, Agostini P, Miller T A, DiMauro L F and Lin C D 2012 *Nature* **483** 194
[16] Wolter B *et al* 2016 *Science* **354** 308
[17] Krausz F and Ivanov M 2009 *Rev. Mod. Phys.* **81** 163
[18] Zhao K, Zhang Q, Chini M, Wu Y, Wang X and Chang Z 2012 *Opt. Lett.* **37** 3891
[19] Li J *et al* 2017 *Nat. Commun.* **8** 186
[20] Gaumnitz T, Jain A, Pertot Y, Huppert M, Jordan I, Ardana-Lamas F and Wörner H J 2017 *Opt. Express* **25** 27506
[21] Kroger L A and Reich C W 1976 *Nucl. Phys.* A **259** 29
[22] Reich C W and Helmer R G 1990 *Phys. Rev. Lett.* **64** 271
[23] Helmer R G and Reich C W 1994 *Phys. Rev.* C **49** 1845
[24] Beck B R *et al* 2007 *Phys. Rev. Lett.* **98** 142501
[25] Seiferle B *et al* 2019 *Nature* **573** 243
[26] Peik E and Tamm C 2003 *Europhys. Lett.* **61** 181
[27] Peik E, Zimmermann K, Okhapkin M and Tamm C 2009 *Proc. 7th Symp. on Frequency Standards and Metrology* ed L Maleki (Singapore: World Scientific) pp 532–8
[28] Rellergert W G, DeMille D, Greco R R, Hehlen M P, Torgerson J R and Hudson E R 2010 *Phys. Rev. Lett.* **104** 200802
[29] Campbell C J, Radnaev A G, Kuzmich A, Dzuba V A, Flambaum V V and Derevianko A 2012 *Phys. Rev. Lett.* **108** 120802
[30] Tkalya E V 2011 *Phys. Rev. Lett.* **106** 162501
[31] Flambaum V V 2006 *Phys. Rev. Lett.* **97** 092502
[32] Berengut J C, Dzuba V A, Flambaum V V and Porsev S G 2009 *Phys. Rev. Lett.* **102** 210801
[33] Fadeev P, Berengut J C and Flambaum V V 2020 *Phys. Rev.* A **102** 052833
[34] Kulander K C, Schafer K J and Krause J L 1993 *Super-Intense Laser-Atom Physics* ed B Piraux, A L'Huillier and K Rzazewski (New York: Plenum)
[35] Schafer K J, Yang B, DiMauro L F and Kulander K C 1993 *Phys. Rev. Lett.* **70** 1599
[36] Corkum P B 1993 *Phys. Rev. Lett.* **71** 1994
[37] Corkum P B 2011 *Phys. Today* **64** 36
[38] Keldysh L V 1965 *Sov. Phys. JETP* **20** 1307

[39] Ammosov M V, Delone N B and Krainov V P 1986 *Sov. Phys. JETP* **64** 1191
[40] van Linden van den Heuvell H B and Muller H G 1988 *Multiphoton Processes* ed S J Smith and P L Knight (Cambridge: Cambridge University Press)
[41] von der Wense L *et al* 2016 *Nature* **533** 47
[42] Yamaguchi A *et al* 2019 *Phys. Rev. Lett.* **123** 222501
[43] Sikorsky T *et al* 2020 *Phys. Rev. Lett.* **125** 142503
[44] Thielking J, Okhapkin M V, Głowacki P, Meier D M, von der Wense L, Seiferle B, Düllmann C E, Thirolf P G and Peik E 2018 *Nature* **556** 321
[45] Minkov N and Pálffy A 2019 *Phys. Rev. Lett.* **122** 162502
[46] Jeet J, Schneider C, Sullivan S T, Rellergert W G, Mirzadeh S, Cassanho A, Jenssen H P, Tkalya E V and Hudson E R 2015 *Phys. Rev. Lett.* **114** 253001
[47] Yamaguchi A, Kolbe M, Kaser H, Reichel T, Gottwald A and Peik E 2015 *New J. Phys.* **17** 053053
[48] Peik E and Okhapkin M 2015 *C. R. Phys.* **16** 516
[49] Stellmer S *et al* 2018 *Phys. Rev.* A **97** 062506
[50] Porsev S G, Flambaum V V, Peik E and Tamm C 2010 *Phys. Rev. Lett.* **105** 182501
[51] Borisyuk P V *et al* 2019 *Phys. Rev.* C **100** 044306
[52] Bilous P V, Bekker H, Berengut J C, Seiferle B, von der Wense L, Thirolf P G, Pfeifer T, López-Urrutia J R C and Pálffy A 2020 *Phys. Rev. Lett.* **124** 192502
[53] Nickerson B S, Pimon M, Bilous P V, Gugler J, Beeks K, Sikorsky T, Mohn P, Schumm T and Pálffy A 2020 *Phys. Rev. Lett.* **125** 032501
[54] Masuda T *et al* 2019 *Nature* **573** 238
[55] Wang W, Zhou J, Liu B and Wang X 2021 *Phys. Rev. Lett.* **127** 052501
[56] Alder K, Bohr A, Huus T, Mottelson B and Winther A 1956 *Rev. Mod. Phys.* **28** 432
[57] Minkov N and Pálffy A 2017 *Phys. Rev. Lett.* **118** 212501
[58] Minkov N and Pálffy A 2021 *Phys. Rev.* C **103** 014313
[59] Grochmalicki J, Lewenstein M and Rzaąewski K 1991 *Phys. Rev. Lett.* **66** 1038
[60] Gajda M, Grochmalicki J, Lewenstein M and Rzążewski K 1992 *Phys. Rev.* A **46** 1638
[61] Brabec T, Ivanov M Y and Corkum P B 1996 *Phys. Rev.* A **54** R2551
[62] Chen J, Liu J, Fu L B and Zheng W M 2000 *Phys. Rev.* A **63** 011404
[63] Yudin G L and Ivanov M Y 2001 *Phys. Rev.* A **63** 033404
[64] Spanner M 2003 *Phys. Rev. Lett.* **90** 233005
[65] Quan W *et al* 2009 *Phys. Rev. Lett.* **103** 093001
[66] Smolarski M, Eckle P, Keller U and Dörner R 2010 *Opt. Express* **18** 17640
[67] Ni H, Saalmann U and Rost J-M 2016 *Phys. Rev. Lett.* **117** 023002
[68] Pullen M G *et al* 2017 *Phys. Rev.* A **96** 033401
[69] Ivanov I A, Nam C H and Kim K T 2017 *Sci. Rep.* **7** 39919
[70] Green A E S, Sellin D L and Zachor A S 1969 *Phys. Rev.* **184** 1–9
[71] Comtois D, Zeidler D, Pépin H, Kieffer J C, Villeneuve D M and Corkum P B 2005 *J. Phys. B: At. Mol. Opt. Phys.* **38** 1923
[72] Pfeiffer A N, Cirelli C, Landsman A S, Smolarski M, Dimitrovski D, Madsen L B and Keller U 2012 *Phys. Rev. Lett.* **109** 083002
[73] Camus N *et al* 2017 *Phys. Rev. Lett.* **119** 023201
[74] Tian J, Wang X and Eberly J H 2017 *Phys. Rev. Lett.* **118** 213201
[75] Wang X, Tian J and Eberly J H 2018 *J. Phys. B: At. Mol. Opt. Phys.* **51** 084002
[76] Xu R, Li T and Wang X 2018 *Phys. Rev.* A **98** 053435
[77] Ivanov M Y, Spanner M and Smirnova O 2005 *J. Mod. Opt.* **52** 165
[78] Radhakrishnan K and Hindmarsh A C 1993 *LLNL Report UCRL-ID-113855* Lawrence Livermore National Laboratory
[79] Baudisch M, Wolter B, Pullen M, Hemmer M and Biegert J 2016 *Opt. Lett.* **41** 3583
[80] Elu U, Baudisch M, Pires H, Tani F, Frosz M H, Köttig F, Ermolov A, Russell P S J and Biegert J 2017 *Optica* **4** 1024
[81] Luu T T, Scagnoli V, Saha S, Heyderman L J and Wörner H J 2018 *Opt. Lett.* **43** 1790
[82] Pupeikis J, Chevreuil P-A, Bigler N, Gallmann L, Phillips C R and Keller U 2020 *Optica* **7** 168
[83] Hammerland D *et al* 2019 *J. Phys. B: At. Mol. Opt. Phys.* **52** 23LT01
[84] Bartels R, Backus S, Zeek E, Misoguti L, Vdovin G, Christov I P, Murnane M M and Kapteyn H C 2000 *Nature* **406** 164
[85] Chipperfield L E, Robinson J S, Tisch J W G and Marangos J P 2009 *Phys. Rev. Lett.* **102** 063003
[86] Jin C, Wang G, Wei H, Le A-T and Lin C D 2014 *Nat. Commun.* **5** 4003
[87] Wang X, Jin C and Lin C D 2014 *Phys. Rev.* A **90** 023416
[88] Andreev A V, Savel'ev A B, Stremoukhov S Y and Shoutova O A 2019 *Phys. Rev.* A **99** 013422
[89] Ghimire S, DiChiara A D, Sistrunk E, Agostini P, DiMauro L F and Reis D A 2011 *Nat. Phys.* **7** 138
[90] Schubert B and Wocker I 2014 *Nat. Photon.* **8** 119
[91] Luu T T, Garg M, Kruchinin S Y, Moulet A, Hassan M T and Goulielmakis E 2015 *Nature* **521** 498
[92] Ndabashimiye G, Ghimire S, Wu M, Browne D A, Schafer K J, Gaarde M B and Reis D A 2016 *Nature* **534** 520
[93] You Y S, Reis D A and Ghimire S 2017 *Nat. Phys.* **13** 345
[94] Yoshikawa N, Tamaya T and Tanaka K 2017 *Science* **356** 736
[95] National Nuclear Data Center 2021 NNDC interactive chart of nuclides https://nndc.bnl.gov/nudat2 (accessed 1 May 2021)